NASA
Technical
Paper
1882

May 1982

Frictional Heating Due to Asperity Interaction of Elastohydrodynamic Line-Contact Surfaces

Bankim C. Majumdar
and Bernard J. Hamrock

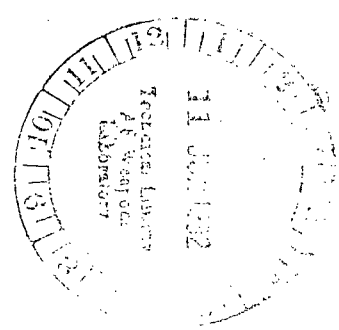

NASA

NASA
Technical
Paper
1882

1982

Frictional Heating Due to Asperity Interaction of Elastohydrodynamic Line-Contact Surfaces

Bankim C. Majumdar
and Bernard J. Hamrock
Lewis Research Center
Cleveland, Ohio

NASA
National Aeronautics
and Space Administration

**Scientific and Technical
Information Branch**

SUMMARY

A numerical solution of an elastohydrodynamically lubricated (EHL) line contact between two long, rough-surface cylinders that considers the frictional heating of asperities was obtained. Pressure distribution, temperature distribution, film thickness and EHL load for given speeds, lubricant properties, material properties of surfaces, and surface roughness parameters were theoretically solved by simultaneous solution of the elasticity equation and the Reynolds equation for two partially lubricated rough surfaces. The pressure due to asperity contact was calculated by assuming a Gaussian distribution of surface irregularities. The elastic deformation used for film thickness computation was found from the two kinds of pressure by plane strain analysis. The temperature rise in the contact zone was calculated by using the Blok-Jaeger flash temperature model. The effect of surface roughness on EHL load for various slide-roll ratios, surface roughness parameters, surface patterns, and temperature parameters was studied. It was found (1) that the maximum temperature rise in most cases occurred in the inlet zone and (2) that minimum film thickness decreased and maximum temperature increased as the surface roughness was increased.

INTRODUCTION

In an earlier report (ref. 1) the effect of the surface roughness of an isothermal, elastohydrodynamically lubricated (EHL) line contact was presented. In heavily loaded, nonconformal machine elements under elastohydrodynamic lubrication there is a possibility of mutual interference between the two surfaces. Although some energy is introduced in an elastohydrodynamically lubricated contact by viscous heating and compression of the lubricant, the predominant thermal energy source is frictional dissipation due to asperity interaction. Frictional heating in the thin-film zone increases the temperature and consequently decreases the viscosity of the lubricant. This gives rise to a reduction in the film thickness. If the temperature is high enough, the lubricating film can fail. Hence the study of the thermal effect in concentrated contacts is important.

Probably Blok (ref. 2) was the first person to use the concept of the flash temperature of a solid as it passes through a heat source. Subsequently Jaeger (ref. 3) presented a theory for estimating flash temperature, and Archard (ref. 4) gave a procedure for determining this temperature. A theoretical study on the thermal stability of such a problem has been made by Christensen (ref. 5). He showed that there was a possibility of thermal instability because of the reduction in film thickness and the increase in the degree of interference of the surfaces. Dyson (ref. 6) discussed various models of the thermal instability of rough-surface contacts. More recently Patir and Cheng (ref. 7) gave a solution for the inlet region of an EHL line-contact problem that considered surface roughness and temperature effects.

Experimental studies on the temperature effect in an EHL contact have been performed by Orcutt (ref. 8), Hamilton and Moore (ref. 9), and Kannel and Bell (ref. 10). They (refs. 8 to 10) used a platinum wire as the temperature transducer and measured the temperature of smooth surfaces in line contact. Hamilton and Moore (ref. 9) found that the maximum temperature rise was always at the inlet zone. Kannel and Bell (ref. 10) used a more sophisticated transducer and measured both pressure and temperature. Winer and his coworkers (refs. 11 to 13) developed an infrared emission technique

to measure the temperatures in sliding and rolling contacts for both smooth and rough surfaces. The experiments showed that the temperature in the inlet zone could be as much as 40° C above ambient temperature.

The present study estimates the minimum film thickness and the contribution of energy dissipation and load for an EHL line contact while taking into consideration the surface roughness effect. Although the method of solution is similar to that of reference 1 it considers the variation of viscosity due to temperature rise caused by frictional heating. Viscous heating and heating due to the compressibility of the lubricant are neglected. The effects of sliding as well as rolling speeds, roughness parameters, load, lubricant properties, material properties, and the roughness patterns of EHL line contacts are investigated.

SYMBOLS

B,b	half the Hertzian contact length, $B = b/R$, m
c	specific heat of metal surface, J/kg K
E_a,E_b	modulus of elasticity of material of surfaces a and b, N/m^2
E'	composite modulus of elasticity, $1/E' = 1/2\,[(1 - \nu_a^2)/E_a + (1 - \nu_b^2)/E_b]$, N/m^2
G	materials parameter, $G = \alpha E'$
H,h	nominal film thickness, $H = h/R$, m
H_{min},h_{min}	minimum film thickness, $H_{min} = h_{min}/R$, m
H_0,h_0	central film thickness, $H_o = h_o/R$, m
h_T	average film thickness, m
K	a constant
k	thermal conductivity of metal, J/m K s
P,p	mean hydrodynamic pressure, $P = p/E'$, N/m^2
P_c,p_c	contact pressure, $P_c = p_c/E'$, N/m^2
Q,q	modified pressure, $Q = q/E'$, N/m^2
R	equivalent radius of cylinder pair, $1/R = (1/R_a) + (1/R_b)$, m
R_a,R_b	radii of cylinders a and b, m
R_s	slide-roll ratio, $R_s = u_s/u$
T	temperature, K
T_0	temperature of oil at inlet condition, K
T_b	a constant, $T_b = (\beta_0)/(T_0 + \beta_1)$
T_c	heating parameter, $T_c = 2\mu\lvert u_s\rvert\sqrt{R}\,E'/[\beta_0\sqrt{\pi\rho ck}\,x\,(\sqrt{u_a} + \sqrt{u_b})]$
$u,u_a,u_b,$ U,U_s,u_s	velocity of surfaces, $u = (u_a + u_b)/2$; $u_s = (u_a - u_b)/2$; $U = \eta_0 u/E'R$; $U_s = \eta_0 u_s/E'R$, m/s
V,v	elastic deformation of surfaces, $V = v/R$, m
V_{ra},V_{rb}	variance ratios, $(\sigma_a/\sigma)^2$, $(\sigma_b/\sigma)^2$
W_c,w_c	asperity contact load per unit length, $W_c = w_c/E'R$, N/m
W_h,w_h	hydrodynamic load per unit length, $W_h = w_h/E'R$, N/m
W_T,w_T	total EHL load per unit length, $W_T = w_T/E'R$; $W_T = W_h + W_c$, N/m
s,x,y,z $S,X,\bar{X}$	coordinates, $S = s/R$; $X = x/R$; $\bar{X} = x/b$, m
α	pressure-viscosity coefficient, m^2/N
β	mean radius of curvature of asperities, m
β_0,β_1	constants, K
γ	surface pattern parameter

γ_a, γ_b	surface pattern parameter of surfaces a and b
η, η_0, η_1	coefficient of absolute viscosity of lubricant, η_0 = the same at inlet condition; η_1 = a constant, N s/m^2
μ	coefficient of friction between interacting asperities
θ	dimensionless temperature rise, $\theta = T/\beta_0$
Λ	hydrodynamic roughness parameter, $\Lambda = h_0/\sigma$
ρ	mass density of metal, kg/m^3
$\sigma, \sigma_a, \sigma_b$	standard deviations of roughness amplitude of surfaces a and b, $\sigma = \sqrt{\sigma_a^2 + \sigma_b^2}$
Φ_s	shear flow factor associated with a single surface
φ_x, φ_y	pressure flow factors
φ_s	shear flow factor associated with two surfaces
ν_a, ν_b	Poisson's ratio of material of surfaces a and b

THEORY

For the EHL contact shown in figure 1 the mean hydrodynamic pressure and asperity contact pressure are to be determined for various input conditions such as loads, speeds, materials, lubricants, and inlet lubricant temperatures.

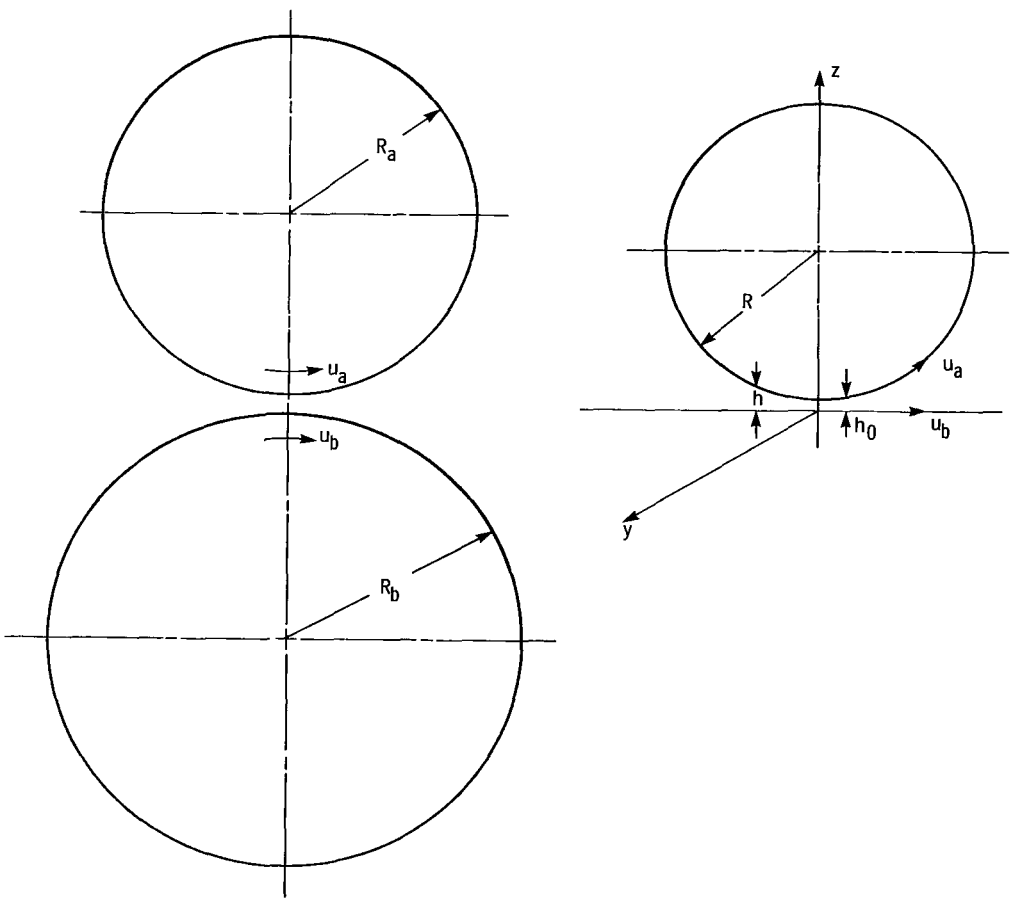

(a) Two heavily loaded, long rough-surface cylinders. (b) Equivalent cylinder near a plane.

Figure 1. - Elastohydrodynamic contact.

The mean hydrodynamic pressure is found from the simultaneous solution of the average Reynolds equation and the elasticity equation. The governing equation for hydrodynamic pressure for rough surfaces when side leakage and local squeeze terms are neglected can be written as (ref. 7)

$$\frac{\partial}{\partial x}\left(\varphi_x \frac{h^3}{12\eta}\frac{\partial p}{\partial x}\right) = \frac{u_a + u_b}{2}\frac{\partial h_T}{\partial x} + \frac{u_a - u_b}{2}\sigma\frac{\partial \varphi_s}{\partial x} \tag{1}$$

where

φ_x pressure flow factor
h_T average gap
σ standard deviation
φ_s shear flow factor

and H_T is given by

$$h_T = \int_{-h}^{\infty} (h + \delta) f(\delta) d\delta \tag{2}$$

where $f(\delta)$ is the probability density function of combined roughness δ. The nominal film thickness h for this type of contact is approximately given by

$$h = h_0 + \frac{x^2}{2R} + v \tag{3}$$

where

h_0 central film thickness
R equivalent radius of curvature of the pair of cylinders
v elastic deformation of cylinders

The coefficient of dynamic viscosity η is assumed to be varied with pressure and temperature according to the following expressions:

$$\eta = \eta_1 e^{\alpha p} \tag{4}$$

and

$$\eta_1 = \eta_0 \exp\left(\frac{\beta_0}{T + \beta_1} - \frac{\beta_0}{T_0 + \beta_1}\right) \tag{5}$$

where

α pressure-viscosity coefficient
η_0 viscosity at inlet condition where the pressure is atmospheric
β_0, β_1 constants

T $T_0 + \Delta T$
T_0 inlet temperature
ΔT rise in temperature

By using equation (4) and letting $(u_a + u_b)/2 = u$ and $(u_a - u_b)/2 = u_s$, equation (1) can be written as

$$\frac{\partial}{\partial x}\left(\varphi_x \frac{h^3}{\eta_1}\frac{\partial q}{\partial x}\right) = 12u\frac{\partial h_T}{\partial x} + 12u_s\sigma\frac{\partial \varphi_s}{\partial x} \tag{6}$$

where

$$q = \frac{1 - e^{-\alpha p}}{\alpha} \tag{7}$$

The pressure flow and shear flow factors φ_x and φ_s have been found by Patir and Cheng (ref. 14) through flow simulation of rough surfaces having Gaussian distribution of surface height. The φ_x for various roughness patterns is given by the following empirical relationship:

$$\left.\begin{aligned} \varphi_x &= 1 - C\, e^{-r(h/\sigma)} \qquad \text{for} \quad \gamma \le 1 \\ &\text{and} \\ \varphi_x &= 1 + C\left(\frac{h}{\sigma}\right)^{-r} \qquad \text{for} \quad \gamma > 1 \end{aligned}\right\} \tag{8}$$

where C and r are constants and can be found in reference 14. The shear flow factor φ_s is a function of h/σ, the standard deviations, and the surface patterns of the surfaces a and b. Patir and Cheng (ref. 14) have shown that the shear flow factor φ_s varies linearly with $(\sigma_a/\sigma)^2$ and $(\sigma_b/\sigma)^2$ and can be expressed in the following form:

$$\varphi_s = \left(\frac{\sigma_a}{\sigma}\right)^2 \Phi_s\left(\frac{h}{\sigma}, \gamma_a\right) - \left(\frac{\sigma_b}{\sigma}\right)^2 \Phi_s\left(\frac{h}{\sigma}, \gamma\right) \tag{9}$$

The Φ_s is given by

$$\Phi_s = A_1\left(\frac{h}{\sigma}\right)^{\alpha_1} \exp\left[-\alpha_2\left(\frac{h}{\sigma}\right) + \alpha_3\left(\frac{h}{\sigma}\right)^2\right] \qquad \text{for} \quad \frac{h}{\sigma} \le 5$$

and

$$\varphi_s = A_2\, e^{-\alpha_4(h/\sigma)} \qquad \text{for} \quad \frac{h}{\sigma} > 5$$

where A_1, A_2, α_1, α_2, α_3, and α_4 are constants that can be found in reference 14.

The ratios $(\sigma_a/\sigma)^2$ and $(\sigma_b/\sigma)^2$ are called the variance ratios of surfaces a and b and are denoted by V_{ra} and V_{rb}, respectively. The variance ratio of surface a can be written as

$$V_{ra} = \left(\frac{\sigma_a}{\sigma}\right)^2 = 1 - \left(\frac{\sigma_b}{\sigma}\right)^2 \tag{10}$$

since

$$\sigma = \sqrt{\sigma_a^2 + \sigma_b^2}$$

If both surfaces have the same surface pattern parameter, equation (9) reduces to

$$\Phi_s = (V_{ra} - V_{rb})\Phi_s\left(\frac{h}{\sigma}, \gamma\right) \tag{11}$$

By combining equations (10) and (11), φ_s can be expressed as

$$\varphi_s = (2V_{ra} - 1)\Phi_s\left(\frac{h}{\sigma}, \gamma\right) \tag{12}$$

When there is sliding, the effect of Φ_s comes into the picture and V_{ra} becomes a parameter. If one of the surfaces is smooth, Φ_s is either a positive or a negative quantity. The physical significance of Φ_s becomes clearer when the significance of the three values of variance ratio, namely, $V_{ra} = 1$, 0.5, and 0, is understood. The variance ratio $V_{ra} = 1$ corresponds to the case shown in figure 2(a), where the rough surface is moving faster

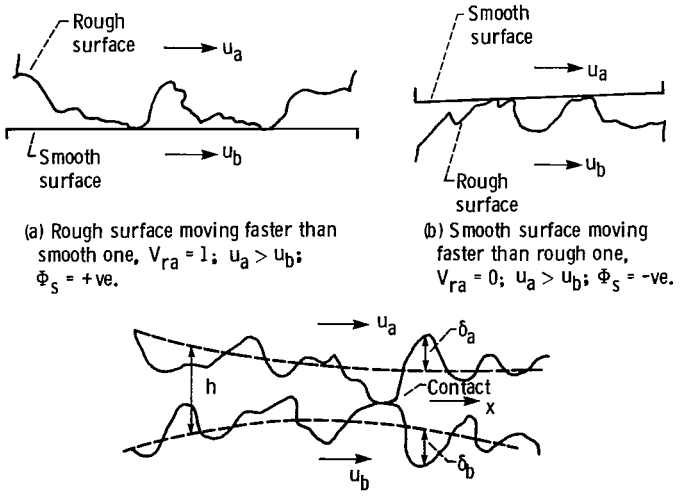

(a) Rough surface moving faster than smooth one, $V_{ra} = 1$; $u_a > u_b$; Φ_s = +ve.

(b) Smooth surface moving faster than rough one, $V_{ra} = 0$; $u_a > u_b$; Φ_s = -ve.

(c) Two surfaces have equal roughness, $V_{ra} = 0.5$; $u_a = u_b$; $\Phi_s = 0$.

Figure 2. - Surface roughness configurations in sliding.

than the smooth one. Conversely, $V_{ra} = 0$ represents a case where the smooth surface is moving faster than the rough one (fig. 2(b)). And when $V_{ra} = 0.5$, the two surfaces have equal roughnesses (i.e., $\sigma_a = \sigma_b$), $\Phi_s = 0$ (fig. 2(c)).

Introducing equation (12) in to equation (6), we get

$$\frac{\partial}{\partial x}\left(\varphi_x \frac{h^3}{\eta_1}\frac{\partial q}{\partial x}\right) = 12u\frac{\partial h_T}{\partial x} + 12u_s\sigma(2V_{ra} - 1)\frac{\partial \Phi_s}{\partial x} \tag{13}$$

It is shown in reference 1 that the expression for $\partial h_T/\partial x$ can be written in terms of nominal film thickness h as

$$\frac{\partial h_T}{\partial x} = \frac{1}{2}\left[1 + \operatorname{erf}\left(\frac{h}{\sqrt{2}\sigma}\right)\right]\frac{\partial h}{\partial x} \tag{14}$$

Substitution of $\partial h_T/\partial x$ into equation (13) yields

$$\frac{\partial}{\partial x}\varphi_x \frac{h^3}{\eta_1}\frac{\partial q}{\partial x} = 12u\frac{1}{2}\left[1 + \operatorname{erf}\left(\frac{h}{\sqrt{2}\sigma}\right)\right]\frac{\partial h}{\partial x} + 12u_s\sigma(2V_{ra} - 1)\frac{\partial \Phi_s}{\partial x} \tag{15}$$

By using the substitutions $X = x/R$, $H = h/R$, $Q = q/E'$, $\Lambda = h_0/\sigma$, and $H_0 = h_0/R$, equation (15) is nondimensionalized. The dimensionless form of equation (15) is written as

$$\frac{\partial}{\partial X}\left(\varphi_x \frac{H^3}{\eta_1}\frac{\partial Q}{\partial X}\right) = 12\frac{u}{E'R}\frac{1}{2}\left[1 + \operatorname{erf}\left(\frac{\Lambda H}{\sqrt{2}\,H_0}\right)\right]\frac{\partial H}{\partial X} + 12\frac{u_s}{E'R}\left(\frac{H_0}{\Lambda}\right)(2V_{ra} - 1)\frac{\partial \Phi_s}{\partial X} \tag{16}$$

To express η_1 in terms of η_0, the effect of temperature on viscosity has to be considered.

Let us now put $\theta = (\Delta T/\beta_0)$ into equation (5). The expression for η_1 then can be written as

$$\eta_1 = \eta_0 \exp\left[T_b\left(\frac{1}{1 + T_b\theta} - 1\right)\right] \tag{17}$$

where

$$T_b = \frac{\beta_0}{T_0 + \beta_1}$$

Substituting equation (17) into equation (16) yields

$$\frac{\partial}{\partial X}\left(\varphi_x H^3 \frac{\partial Q}{\partial X}\right) - \frac{\eta_0}{\eta_1^2}\varphi_2 H^3 \frac{\partial Q}{\partial X}\frac{\partial \eta_1}{\partial X} = 12U\left\{\frac{1}{2}\left[1 + \operatorname{erf}\left(\frac{\Lambda H}{\sqrt{2}\,H_0}\right)\right]\frac{\partial H}{\partial X}\right.$$

$$\left. + R_s\left(\frac{H_0}{\Lambda}\right)(2V_{ra} - 1)\frac{\partial \Phi_s}{\partial X}\right\}\exp\left[T_b\left(\frac{1}{1 + T_b\theta} - 1\right)\right] \tag{18}$$

where

$$U = \frac{\eta_0 u}{E' R}$$

and

$$R_s = \frac{u_s}{u}$$

Equation (18) can also be written in the following form:

$$\frac{\partial}{\partial X}\left(\varphi_x H^3 \frac{\partial Q}{\partial X}\right) + \exp\left[-T_b\left(\frac{1}{1 + T_b\theta} - 1\right)\right] \times \frac{T_b^2}{(1 + T_b\theta)^2}\varphi_x H^3 \frac{\partial Q}{\partial X}\frac{\partial \theta}{\partial X}$$

$$= 12u\left\{\frac{1}{2}\left[1 + \operatorname{erf}\left(\frac{\Lambda H}{\sqrt{2}\,H_0}\right)\right]\frac{\partial H}{\partial X} + R_s\left(\frac{H_0}{\Lambda}\right)(2V_{ra} - 1)\frac{\partial \Phi_s}{\partial X}\right\}\exp\left[T_b\left(\frac{1}{1 + T_b\theta} - 1\right)\right] \tag{19}$$

To know H, we have to find the elastic deformation of the cylinders. The deformation v is calculated for a semi-infinite solid in a state of plane strain. The equation of deformation for two cylinders is (ref. 1)

$$V(X) = -\frac{4}{\pi}\int_{S_1}^{S_2}(P + P_c)\ln|X - S|\,dS \tag{20}$$

where

$$V = \frac{v}{R}$$

and

$$S = \frac{s}{R}$$

The procedure for calculating V is shown in detail in reference 1. After V is introduced in equation (3), the dimensionless film thickness H will be given by

$$H = H_0 + \frac{X^2}{2} + V \tag{21}$$

Before finding a solution of equation (19) for particular values of Λ, H_0, U, R_s, and T_b, we must express θ in terms of X. Using the modified form of Blok's flash temperature model (ref. 7), we can express the temperature rise θ ($= \Delta T/\beta_0$) by the equation

$$\theta(X) = T_c \int_{S_1}^{S_2} \frac{P_c(S)}{\sqrt{X - S}}\, dS \tag{22}$$

where

$$T_c = \frac{2\mu |u_s| \sqrt{R}\, E'}{\beta_0 \sqrt{\pi \rho c k}\left(\sqrt{u_a} + \sqrt{u_b}\right)}$$

and P_c is the dimensionless contact pressure, $P_c = p_c/E'$. Therefore θ can be obtained after evaluating the contact pressure. The contact pressure has been estimated by using a method given by Greenwood and Tripp (ref. 15) and by reference 1.

Now knowing H, φ_X, and θ, we can solve equation (14) by finite difference methods for given values of G, U, R_s, Λ, H_0, T_b, and T_c. The boundary conditions used are Reynolds boundary conditions. The details of the method can be found in reference 1. The Q distribution is transformed to P distribution from

$$P = -\frac{1}{G} \ln (1 - GQ) \tag{23}$$

Having obtained the pressure distribution, we can calculate the hydrodynamic load from

$$w_h = \int_{s_1}^{s_2} p\, dx \tag{24}$$

or

$$W_h = -\frac{1}{G} \int_{S_1}^{S_2} \ln(1 - GQ)\, dX \tag{25}$$

where

$$W_h = \frac{w_h}{E'R}$$

The contact load is

$$w_c = \int_{-b}^{b} p_c\, dx \tag{26}$$

or

$$W_c = \int_{-B}^{B} P_c\, dX \tag{27}$$

where

$$B = \frac{b}{R}$$

and

$$W_c = \frac{w_c}{E'R}$$

The integrations of equations (25) and (27) are performed numerically by Simpson's rule. The total dimensionless EHL load W_T is

$$W_T = \frac{w_T}{E'R} \tag{28}$$

where

$$w_T = w_c + w_h$$

RESULTS AND DISCUSSION

From the theory it can be seen that there are two kinds of dimensionless parameters - parameters relating to EHL and those due to the surface roughness effect including frictional heating. The EHL parameters are W_h, U, H, R_s, and G. The other parameters are W_c, Λ, V_{ra}, σ/β, γ, T_c, and T_b. Thus both film thickness and temperature are functions of W_T, U, R_s, G, Λ,

V_{ra}, σ/β, γ, T_c and T_b. From the foregoing theory EHL load, film thickness and temperature rise were calculated for various speeds, slide-roll ratios, roughness parameters, variance ratios, surface patterns, and heating and materials parameters and are presented in figures 3 to 12 and tables I to III. The parameters G, U, R_s, Λ, σ/β, V_{ra}, and T_c cover a wide range of practical situations. In the following paragraphs the effect of some of these parameters is discussed.

Effect of Hydrodynamic Roughness Parameter

The total EHL load decreased with increases in the surface roughness (fig. 3). (The smaller the values of Λ, the higher is the surface roughness). The minimum film thickness decreased slightly as the surface roughness was increased (fig. 4), and the maximum temperature rise increased with increases in the surface roughness (fig. 5). The variation of EHL load, minimum film thickness, and maximum temperature with the roughness parameter Λ for various materials parameters G is also shown in figures 3 to 5 for certain input conditions. The trend of EHL load and minimum film thickness with U, G, and Λ was found to be similar to that observed when the temperature effect was not considered (ref. 1). In figure 6 the distribution of temperature rise is plotted for two roughness parameters (Λ = 1 and 2) and two materials parameters (G = 5000 and 7500). The maximum temperature rise always occurred in the inlet zone of the Hertzian contact. Similar observations have been made experimentally by Hamilton and Moore (ref. 9). Although in reference 11 it was given that the maximum temperature rise would occur nearly in the exit zone, Jaeger (ref. 3) showed that his model could give the minimum temperature rise in the inlet zone.

Effect of Variance Ratio V_{ra}

The EHL load, minimum film thickness, and maximum temperature rise are plotted in figures 7 to 9 for three variance ratios (V_{ra} = 1, 0.5, and 0). The EHL load did not change significantly when V_{ra} changed from 0 to 0.5. But when the rough surface was moving faster than the smooth one (i.e., when V_{ra} = 1.0), the EHL load dropped (fig. 7). However, there was little or no variation in minimum film thickness with the change of variance ratio (fig. 8). The temperature rise was highest for V_{ra} = 1.0, lowest for V_{ra} = 0.5, and intermediate for V_{ra} = 0 (fig. 9).

Effect of Surface Pattern Parameter γ

In figures 10 to 12 the variations in EHL load, minimum film thickness, and maximum temperature rise are shown for various surface pattern parameters. The surface pattern parameters γ of 1/6, 1, and 6 represent transversely oriented, isotropic, and longitudinally oriented surfaces, respectively. For a particular set of input conditions, longitudinally and transversely oriented surfaces gave maximum and minimum EHL load, respectively (fig. 10). The smallest value of minimum film thickness was obtained for isotropic surfaces (fig. 11). The maximum temperature rise increased at a steeper rate with increasing Λ for the longitudinally oriented surface (fig. 12). The curves representing γ of 1/6 and 1 are, for all practical purposes, identical.

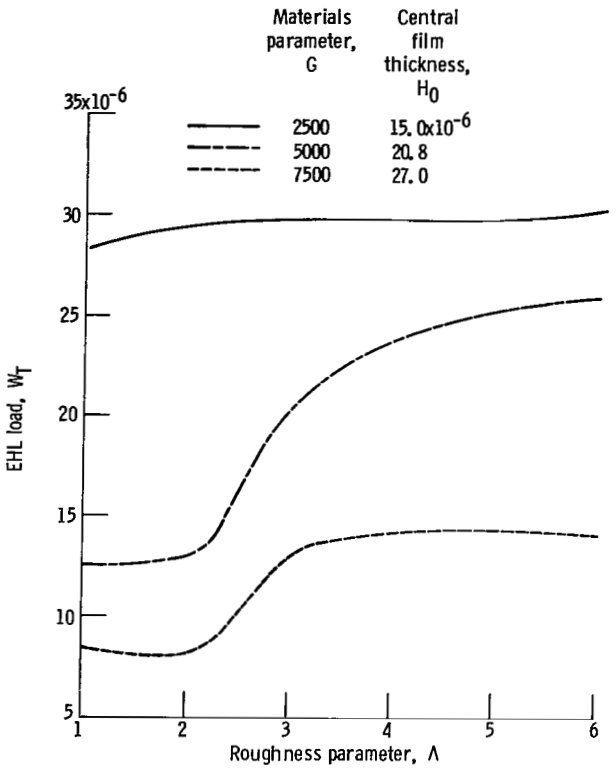

Figure 3. - Variation of EHL load with roughness parameter for various materials parameters. $\gamma = 1$; $\sigma/\beta = 0.0001$; $U = 10^{-11}$ m/s; $R_s = 0.5$; $T_c = 3000$; $T_b = 5$; $V_{ra} = 0.5$.

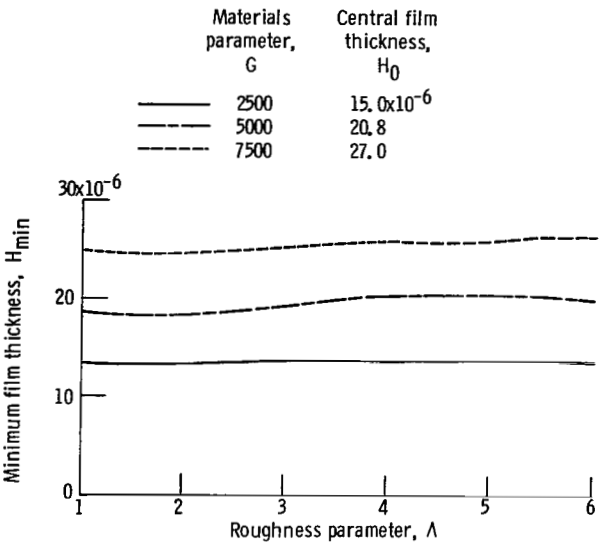

Figure 4. - Variation of minimum film thickness with roughness parameter for various materials parameters. $\gamma = 1$; $\sigma/\beta = 0.0001$; $U = 10^{-11}$ m/s; $R_s = 0.5$; $T_c = 3000$; $T_b = 5$; $V_{ra} = 0.5$.

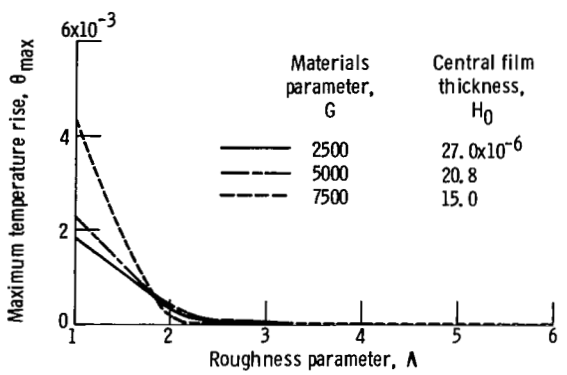

Figure 5. - Variation of maximum temperature rise with roughness parameter for various materials parameters. $\gamma = 1$; $\sigma/\beta = 0.0001$; $U = 10^{-11}$ m/s; $R_s = 0.5$; $T_c = 3000$; $T_b = 5$; $V_{ra} = 0.5$.

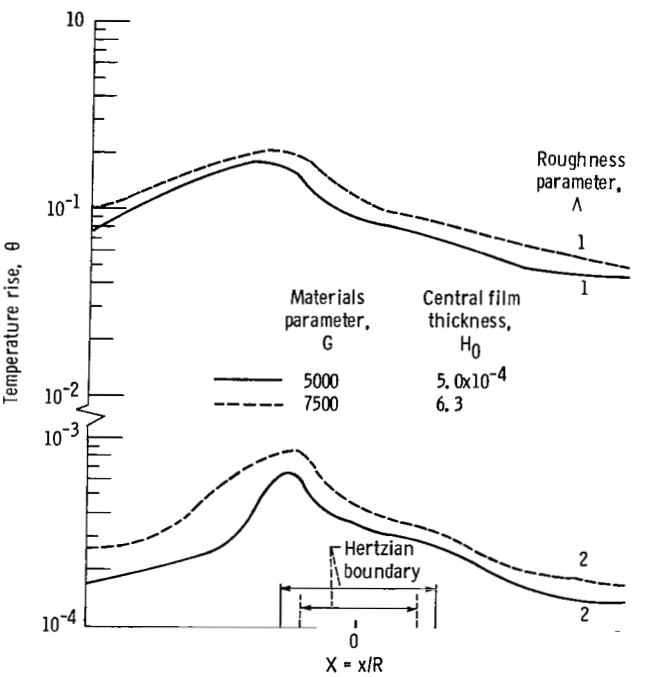

Figure 6. - Temperature distribution in contact zone. $\gamma = 1$; $\sigma/\beta = 0.0001$; $U = 10^{-9}$ m/s; $R_s = 0.5$; $T_c = 3000$; $T_b = 5$; $V_{ra} = 1$.

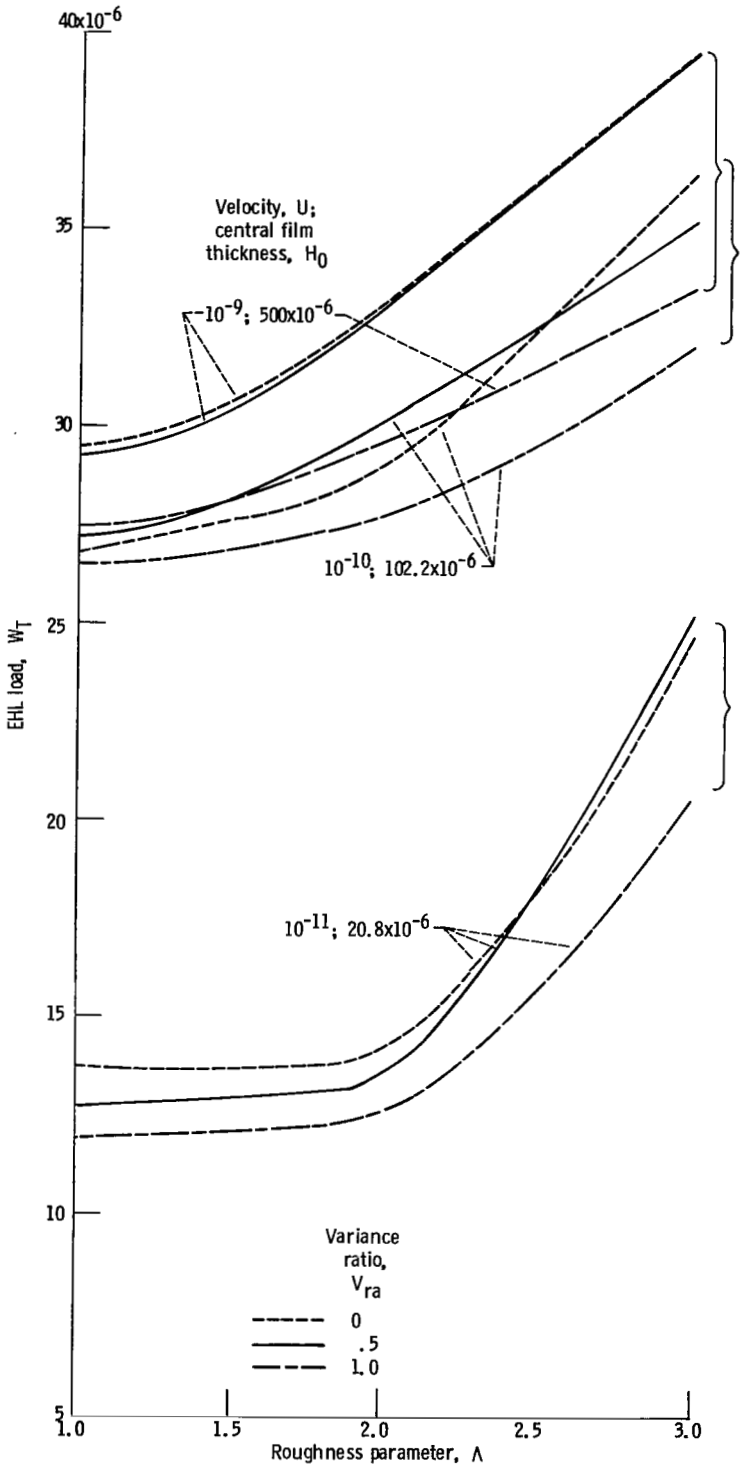

Figure 7. - Variation of EHL load with roughness parameter for various variance ratios. $\gamma = 1$; $G = 5000$; $\sigma/\beta = 0.0001$; $R_s = 0.5$; $T_c = 3000$; $T_b = 5$.

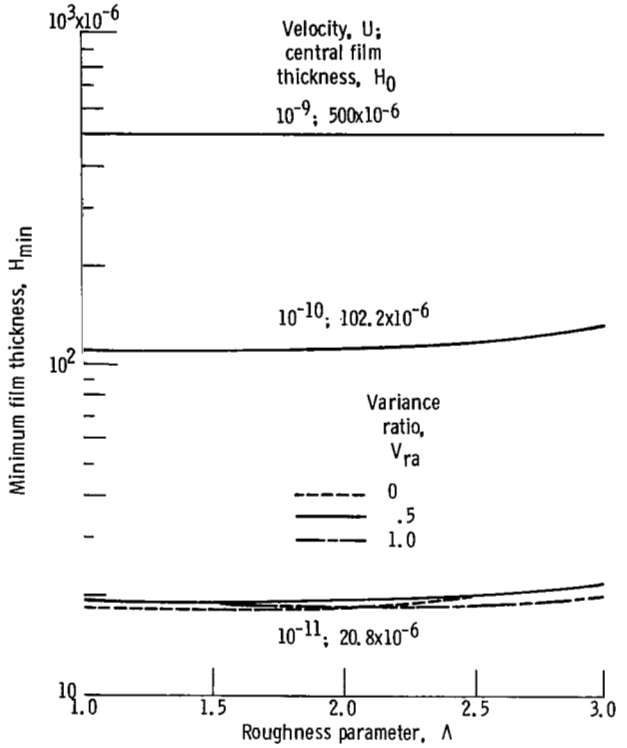

Figure 8. - Variation of minimum film thickness with roughness parameter for various variance ratios. $\gamma = 1$; $G = 5000$; $\sigma/\beta = 0.0001$; $R_s = 0.5$; $T_c = 3000$; $T_b = 5$.

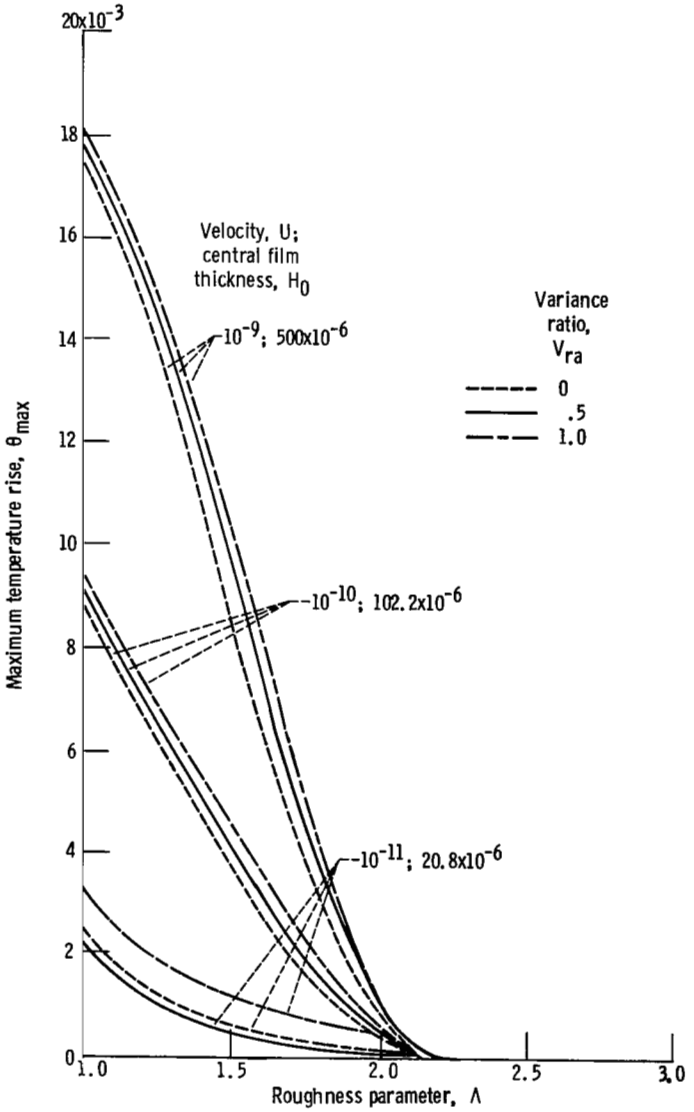

Figure 9. - Variation of maximum temperature rise with roughness parameter for various variance ratios. $\gamma = 1$; $G = 5000$; $\sigma/\beta = 0.0001$; $R_s = 0.5$; $T_c = 3000$; $T_b = 5$.

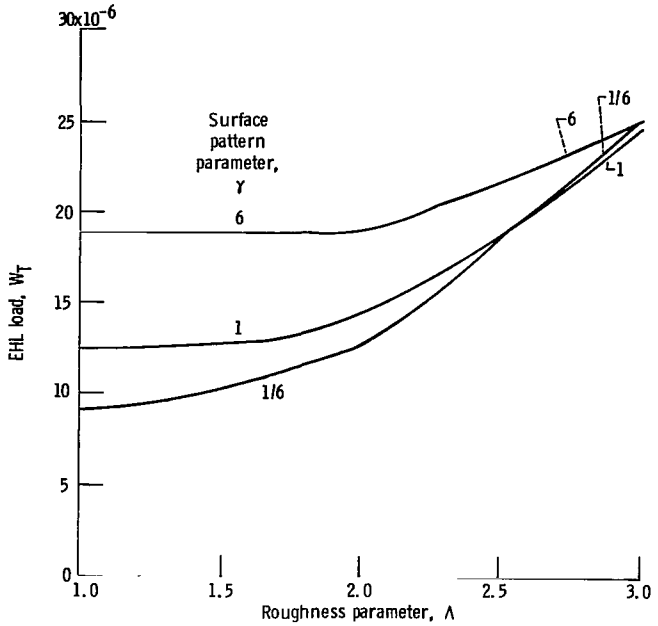

Figure 10. - Variation of EHL load with roughness parameter for various surface patterns. G = 5000; σ/β = 0.0001; R_s = 0.5; T_c = 3000; V_{ra} = 0.5.

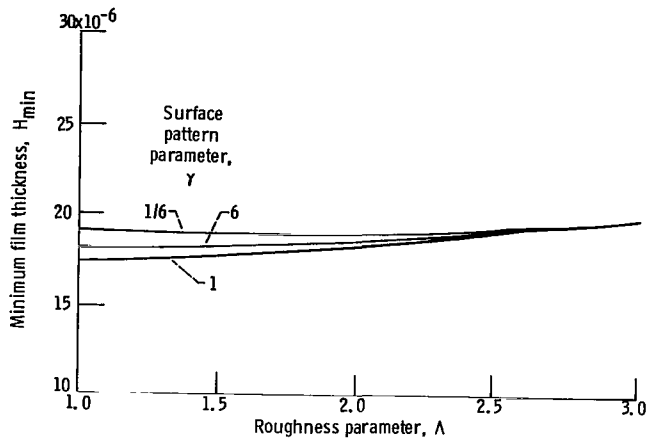

Figure 11. - Variation of minimum film thickness with roughness parameter for various surface patterns. G = 5000; σ/β = 0.0001; R_s = 0.5; T_c = 3000; V_{ra} = 0.5.

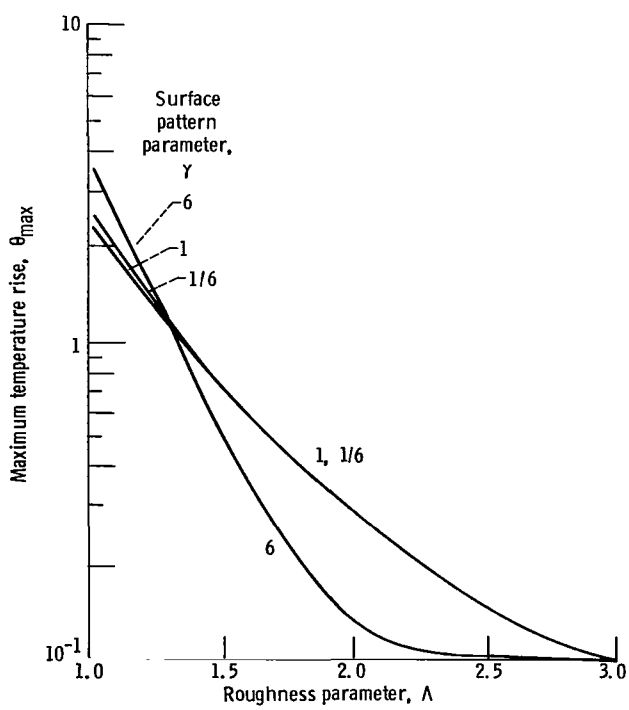

Figure 12. - Variation of maximum temperature rise with roughness parameter for various surface patterns. G = 5000; σ/β = 0.0001; R_s = 0.5; T_c = 3000; T_b = 5; V_{ra} = 0.5.

Effect of Heating Parameter T_C

In table I the variation of minimum film thickness and maximum temperature rise for three heating parameters (T_C = 50, 3000, and 6000) is shown. Although the minimum film thickness did not change appreciably with T_C, the temperatures rose with increases in the heating parameters. This is evident from the physical point of view.

Effect of Surface Contact Roughness Parameter σ/β

The higher the value of σ/β, the rougher is the surface. The rise in maximum temperature increased with increases in the value of σ/β. The minimum film thickness also fell slightly as σ/β was increased (table II).

Effect of Slide-Roll Ratio R_s

The slide-roll ratio $R_s = 0$ corresponds to a pure-rolling case. The effect of R_s on H_{min} and θ_{max} for various V_{ra} is given in table III. When both surfaces had the same roughness structure (i.e., $V_{ra} = 0.5$), both minimum film thickness and maximum temperature rise did not change with the slide-roll ratio. The minimum film thickness decreased as the slide-roll ratio was increased for variance ratios V_{ra} of 0 and 1.0. On the other hand the maximum temperature rise dropped when $V_{ra} = 0$ and increased when $V_{ra} = 1.0$.

EXAMPLE

From the temperature distribution θ it is sometimes difficult to estimate the quantitative value of temperature rise in the contact zone. The following example illustrates a calculation procedure for finding ΔT.

Two heavily loaded cylinders having surface a rough and surface b smooth are lubricated under the following conditions:

Cylinder radii, $R_a = 0.033$ m, $R_b = 0.05$ m
Velocity of surface of cylinder a, $u_a = 9$ m/s
Velocity of surface of cylinder b, $u_b = 4$ m/s
Mean coefficient of friction for a contact between asperities, $\mu = 0.5$
Equivalent modulus of elasticity of cylinder materials,
$E' = 2.2 \times 10^{11}$ N/m^2
Density of material, $\rho = 8 \times 10^3$ kg/m^3
Thermal conductivity of material, k = 10 J/m K s
Specific heat of material, c = 100 J/kg K
Central film thickness, $h_0 = 0.416 \times 10^{-6}$ m
Pressure-viscosity coefficient of lubricant, $\alpha = 2.27 \times 10^{-8}$ m^2/N
Viscosity of lubricant, $\eta_0 = 0.0068$ Pa s

From these data and $\beta_0 = 2050$ K, the following parameters are calculated:

Dimensionless speed parameter.

$$U \cong 10^{-11}$$

TABLE I. - VARIATION OF MINIMUM FILM THICKNESS AND MAXIMUM TEMPERATURE RISE FOR VARIOUS HEATING PARAMETERS

[$\gamma = 1$; $G = 5000$; $\sigma/\beta = 0.0001$; $R_s = 0.5$; $T_b = 5$; $V_{ra} = 0.5$.]

Surface velocity, U, m/s	Cantral film thickness, H_0, m	Hydro-dynamic roughness parameter, Λ	Heating parameter, T_c					
			50		3000		6000	
			Values of minimum film thickness, m, and maximum temperature rise, K					
			H_{min}	θ_{max}	H_{min}	θ_{max}	H_{min}	θ_{max}
10×10^{-12}	20.80×10^{-6}	1	17.96×10^{-6}	0.438×10^{-3}	18.39×10^{-6}	2.597×10^{-3}	17.87×10^{-6}	5.440×10^{-3}
		2	17.76	.003	17.79	.220	17.76	.398
		3	20.23	0	20.23	.001	20.23	.003

TABLE II. - VARIATION OF MINIMUM FILM THICKNESS AND MAXIMUM TEMPERATURE RISE FOR VARIOUS RATIOS OF PRESSURE-VISCOSITY COEFFICIENT TO MEAN RADIUS OF CURVATURE OF ASPERITIES

[$\gamma = 1$; $G = 5000$; $R_s = 0.5$; $T_c = 3000$; $T_b = 5$.]

Surface velocity, U, m/s	Central film thickness, H_0, m	Hydro-dynamic roughness parameter, Λ	$\sigma/\beta = 0.0001$		$\sigma/\beta = 0.01$	
			Values of minimum film thickness, m, and maximum temperature rise, K			
			H_{min}	θ_{max}	H_{min}	θ_{max}
10×10^{-12}	20.80×10^{-6}	1	18.39×10^{-6}	2.289×10^{-3}	18.35×10^{-6}	3.412×10^{-3}
		2	17.79	.220	17.72	.224
		3	20.23	.001	20.39	.014

TABLE III. - VARIATION OF MINIMUM FILM THICKNESS AND MAXIMUM TEMPERATURE FOR VARIOUS SLIDE-ROLL RATIOS AND VARIANCE RATIOS

[γ = 1; G = 5000; σ/β = 0.0001; U = 10^{-11} m/s; H_0 = 20.8×10^{-6} m; T_c = 3000, T_b = 5.]

Variance ratio, V_{ra}	Hydrodynamic roughness parameter, Λ	Slide-roll ratio, R_s			
		0		0.5	
		Values of minimum film thickness, m, and maximum temperature rise, K			
		H_{min}	θ_{max}	H_{min}	θ_{max}
0	1	18.40×10^{-6}	2.397×10^{-3}	17.48×10^{-6}	2.371×10^{-3}
	2	17.79	.223	17.55	.223
	3	20.23	.001	20.25	.001
.5	1	18.40	2.289	18.40	2.289
	2	17.79	.218	17.79	.218
	3	20.23	.001	20.23	.001
1.0	1	18.40	2.289	18.13	3.231
	2	17.79	.218	18.59	.169
	3	20.23	.001	20.11	.002

Dimensionless central film thickness.

$$H_0 = 20.8\times10^{-6}$$

Dimensionless materials parameter.

$$G \cong 5000$$

Heating parameter.

$$T_c \approx 3000$$

Assuming $\gamma = 1$, $\Lambda = 1$, $R_s = 0.5$, $T_b = 5$, and $\sigma/\beta = 0.0001$, we get from figure 9, $\theta_{max} = 3.2\times10^{-3}$. Now the maximum temperature rise $\Delta T_{max} = \theta_{max}\beta_0 = 6.56$ K.

CONCLUSIONS

From the data presented herein the following conclusions were drawn:

1. The elastohydrodynamic load for a constant central film thickness decreases with increasing hydrodynamic surface roughness.
2. Minimum film thickness decreases with increasing roughness.
3. The maximum rise in temperature increases with increasing surface roughness.
4. The location of maximum temperature is always in the inlet zone.

5. The minimum film thickness decreases as the cylinders start sliding from pure rolling.

6. Film thickness and temperature rise are independent of the slide-roll ratio for surfaces with equal roughness structures.

7. When the rough surface is moving faster than the smooth one (variance ratio $V_{ra} = 1$), the temperature increases for higher slide-roll ratios.

8. There is no significant change in minimum film thickness when V_{ra} varies from 0 to 1.

Lewis Research Center
National Aeronautics and Space Administration
Cleveland, Ohio, November 2, 1981

REFERENCES

1. Majumdar, Bankim C.; and Hamrock, Bernard J.: Effect of Surface Roughness on Elastohydrodynamic Line Contact. NASA TM-81753, 1981.
2. Blok, H.: Discussion, paper by K. P. Baglin and J. F. Archard. Elastohydrodynamic Lubrication, 1972 Symposium, Institution of Mechanical Engineers, London, 1972, pp. 163-167.
3. Jaeger, J. C.: Moving Sources of Heat and the Temperature of Sliding Contacts. Proc. R. Soc., N.S.W., vol. 76, 1943, pp. 203-224.
4. Archard, J. F.: The Temperature of Rubbing Surfaces. Wear, vol. 2, no. 6, 1958/1959, pp. 438-455.
5. Christensen, H.: The Reliability of the Elastohydrodynamic Oil Film. First European Tribology Congress, Paper C269/73, 1973 (Institution of Mechanical Engineers, London).
6. Dyson, A.: Thermal Stability of Models of Rough Elastohydrodynamic Systems. J. Mech. Eng. Sci., vol. 18, no. 1, Feb. 1976, pp. 11-18.
7. Patir, N.; and Cheng, H. S.: Effect of Surface Roughness Orientation on the Central Film Thickness in E.H.D. Contacts. Elastohydrodynamics and Related Topics, Proceedings of 5th Leeds-Lyon Symposium on Tribology, Institute of Tribology, D. Dowson, ed., Mechanical Engineering Publications, 1979, pp. 15-21.
8. Orcutt, F. K.. Experimental Study of Elastohydrodynamic Lubrication. ASLE Trans., vol. 8, no. 4, 1965, pp. 381-396.
9. Hamilton, G. M.; and Moore, S. L.: Deformation and Pressure in an Elastohydrodynamic Contact. Proc. R. Soc., London, ser. A, vol. 322, 1971, pp. 313-330.
10. Kannel, J. W.; and Bell, J. C.: A Method for Estimation of Temperature in Lubricated Rolling-Sliding Gear on Bearing Elastohydrodynamic Contacts. Elastohydrodynamic Lubrication, 1972 Symposium, Institution of Mechanical Engineers, London, Paper C24/72, 1972, pp. 118-130.
11. Ausherman, V. K.; et al.: Infrared Temperature Mapping in Elastohydrodynamic Lubrication. J. Lubr. Technol., vol. 98, no. 2, Apr. 1976, pp. 236-243.
12. Nagaraj, H. S.; Sanborn, D. M.; and Winer, W. O.: Direct Surface Temperature Measurement by Infrared Radiation in Elastohydrodynamic Contacts and the Correlation with the Blok Flash Temperature Theory. Wear, vol. 49, no. 1, 1978, pp. 43-59.
13. Winer, W. O.: A Review of Temperature Measurements in EHD Contacts. Elastohydrodynamics and Related Topics, Proceedings of 5th Leeds-Lyon Symposium on Tribology, Institute of Tribology, D. Dowson, ed., Mechanical Engineering Publications, 1979, pp. 125-130.

14. Patir, N.; and Cheng, H. S.: Application of Average Flow Model to Lubrication Between Rough Sliding Surfaces. J. Lubr. Technol., vol. 101, no. 2, Apr. 1979, pp. 220-230.
15. Greenwood, J. A.; and Tripp, J. H.: The Contact of Two Nominally Flat Rough Surfaces. Proc. Inst. Mech. Eng.. London, vol. 185, 1970-71, pp. 625-633.

1. Report No.	2. Government Accession No.	3. Recipient's Catalog No.
NASA TP-1882		

4. Title and Subtitle	5. Report Date
FRICTIONAL HEATING DUE TO ASPERITY INTERACTION OF ELASTOHYDRODYNAMIC LINE-CONTACT SURFACES	May 1982
	6. Performing Organization Code 505-32-42
7. Author(s)	8. Performing Organization Report No.
Bankim C. Majumdar and Bernard J. Hamrock	E-897
	10. Work Unit No.
9. Performing Organization Name and Address	
National Aeronautics and Space Administration Lewis Research Center Cleveland, Ohio 44135	11. Contract or Grant No.
	13. Type of Report and Period Covered
12. Sponsoring Agency Name and Address	Technical Paper
National Aeronautics and Space Administration Washington, D.C. 20546	14. Sponsoring Agency Code

15. Supplementary Notes

Bankim C. Majumdar, Indian Institute of Technology, Khagpur, India and National Research Council - NASA Research Associate; Bernard J. Hamrock, Lewis Research Center. Previously presented at ASME-ASLE Joint Lubrication Conference, October 5-7, 1981, New Orleans, Louisiana.

16. Abstract

A numerical solution of an elastohydrodynamically lubricated (EHL) line contact between two long, rough-surface cylinders that considers the frictional heating of asperities was obtained. Pressure distribution, temperature distribution, film thickness and EHL load for given speeds, lubricant properties, material properties of surfaces, and surface roughness parameters were theoretically solved by simultaneous solution of the elasticity equation and the Reynolds equation for two partially lubricated rough surfaces. The pressure due to asperity contact was calculated by assuming a Gaussian distribution of surface irregularities. The elastic deformation used for film thickness computation was found from the two kinds of pressure by plane strain analysis. The temperature rise in the contact zone was calculated by using the Blok-Jaeger flash temperature model. The effect of surface roughness on EHL load for various slide-roll ratios, surface roughness parameters, surface patterns, and temperature parameters was studied. It was found (1) that the maximum temperature rise in most cases occurred in the inlet zone and (2) that the minimum film thickness decreased and the maximum temperature increased as the surface roughness was increased.

17. Key Words (Suggested by Author(s))	18. Distribution Statement
Elastohydrodynamic lubrication Surface roughness Line contact Temperature rise due to asperity contact	Unclassified - unlimited STAR Category 37

19. Security Classif. (of this report)	20. Security Classif. (of this page)	21. No. of Pages	22. Price*
Unclassified	Unclassified	22	A02

* For sale by the National Technical Information Service, Springfield, Virginia 22161

NASA-Langley, 1982

National Aeronautics and
Space Administration

Washington, D.C.
20546

Official Business
Penalty for Private Use, $300

THIRD-CLASS BULK RATE

Postage and Fees Paid
National Aeronautics and
Space Administration
NASA-451

NASA

POSTMASTER: If Undeliverable (Section 158 Postal Manual) Do Not Return